UCLA
UCLA Previously Published Works

Title

Ischemia-Induced Ventricular Proarrhythmia and Cardiovascular Autonomic Dysreflexia After Cardioneuroablation

Permalink

https://escholarship.org/uc/item/1ch0h02d

Authors

Chung, Wei-Hsin
Masuyama, Kiyoshi
Challita, Ronald
et al.

Publication Date

2023-08-01

DOI

10.1016/j.hrthm.2023.08.001

Copyright Information

This work is made available under the terms of a Creative Commons Attribution License, available at https://creativecommons.org/licenses/by/4.0/

Peer reviewed

eScholarship.org Powered by the California Digital Library
University of California

Ischemia-Induced Ventricular Proarrhythmia and Cardiovascular Autonomic Dysreflexia After Cardioneuroablation

Wei-Hsin Chung, MD[1,2]; Kiyoshi Masuyama MD PhD[1]; Ronald Challita MD[1]; Justin Hayase, MD[1]; Shumpei Mori, MD PhD[1]; Steven Cha BS[1]; Jason S. Bradfield, MD[1]; Jeffery L. Ardell. PhD[1]; Kalyanam Shivkumar, MD, PhD[1] and Olujimi Ajijola, MD, PhD[1]

[1]*UCLA Cardiac Arrhythmia Center, Ronald Reagan UCLA Medical Center, Los Angeles, CA*
[2] *China Medical University Hospital, Taichung, Taiwan*

Running Title: Cardioneuroablation and ventricular arrhythmias

Conflict of interest:

The first author and remaining authors have nothing to disclose.

Corresponding author:

Olujimi Ajijola, MD, PhD
UCLA Cardiac Arrhythmia Center
100 medical Plaza, Suite 660
Los Angeles, CA 90095

Funding statement:
Supported by NIH/NHLBI grant HL159001 to OAA

ABSTRACT

Background
Cardioneuroablation (CNA) is an attractive treatment for vasovagal syncope. Its long-term efficacy and safety remain unknown.

Objective
To develop a chronic porcine model of CNA to examine ventricular tachyarrhythmia (VT/VF) susceptibility and cardiac autonomic function after CNA.

Methods
A percutaneous CNA model was developed by ablation of left- and right-sided ganglionated plexi (GP)(n=5), confirmed by histology. Reproducible bilateral vagal denervation was confirmed following CNA by extracardiac vagal nerve stimulation (ECVNS) and histology. Chronic studies included 16 pigs randomized to CNA (n=8) and sham ablation (n=8). After 6 weeks, animals underwent hemodynamic studies, assessment of cardiac sympathetic and parasympathetic function using sympathetic chain stimulation (SCS) and direct VNS respectively, and proarrhythmic potential following left anterior descending coronary artery (LAD) ligation.

Results
After CNA, ECVNS responses remained abolished for 6 weeks despite ganglia remaining in ablated GPs. In the CNA group, direct VNS resulted in paradoxical increases in blood pressure, but not in sham animals (CNA group vs. sham: 8.36±7.0% vs. -4.83±8.7%, respectively, p=0.009). Left SCS (8Hz) induced significant QTc prolongation in the CNA group vs. sham (11.23±4.0% vs. 1.49±4.0%, respectively, p<0.001). VT/VF after LAD ligation was more prevalent and occurred earlier in the CNA group vs. control (61.44±73.7sec vs. 245.11±104.0 sec, respectively, p=0.002).

Conclusions
Cardiac vagal denervation is maintained long-term after CNA in a porcine model. However, chronic CNA was associated with cardiovascular dysreflexia, diminished cardioprotective effects of cardiac vagal tone, and increased VT/VF susceptibility in ischemia. These potential long-term negative impacts of CNA suggest the need for rigorous clinical studies on CNA.

Condensed abstract
A porcine model of reproducible chronic cardioneuroablation (CNA) was developed. After 6 weeks, the effects of CNA persisted with evidence of autonomic dysregulation and repolarization abnormalities. Attenuated heart rate responses were observed during bilateral extracardiac vagal nerve stimulation. However, a paradoxical left ventricle systolic pressure response occurred in CNA animals. Bilateral sympathetic chain stimulation enhanced QTc interval prolongation in the ablation group. After LAD ligation, the ablation group showed greater susceptibility to ventricular arrhythmias, highlighting the potential negative impact of ganglionated plexi ablation.

Keywords: ganglionated plexi ablation; cardioneuroablation; ventricular arrhythmias; intrinsic cardiac network; dysautonomia; neuromodulation.

Abbreviation list
AF= Atrial Fibrillation
CNA= cardioneuroablation
ECG= electrocardiography
GP= ganglionated plexi
HR= heart rate
(G)HFS= (gated) high-frequency stimulation
LAD= left anterior descending coronary artery
LSCS/RSCS= left sympathetic chain stimulation/ right sympathetic chain stimulation
LSGP= left superior ganglionated plexi
LVNS/RVNS= left vagal nerve stimulation/ right vagal nerve stimulation
RAGP= right atrial ganglionated plexi

INTRODUCTION

Ganglionated plexi (GP), also known as "little brain" in the heart, comprise motor, sensory, and interconnecting neurons that serve as the final regulator of regional cardiac function.[1] The role of GPs in the initiation of atrial fibrillation (AF) led to therapeutic targeting of GPs by radiofrequency ablation,[2] however, this fell out of favor due to inconsistent AF outcomes following GP ablation.[3] Recently, GP ablation has been applied for the management of vasovagal syncope (VVS), commonly known as cardioneuroablation (CNA).[4] Several studies have reported clinical improvement after CNA.[5] Although CNA represents a promising treatment for an otherwise challenging clinical problem, approaches to identify GPs, procedural endpoints, optimal ablation approach, and histological effects of ablation remain poorly understood. Most importantly, the long-term consequences of disrupting the delicate balance of cardiac autonomic nervous control remain unknown.[6] This study aimed to develop a preclinical porcine model of chronic CNA to examine VA susceptibility and autonomic regulation in the intermediate term.

METHODS

Animal studies

This study was performed according to animal care guidelines of both the University of California Institutional Animal Care and Use Committee and the National Institutes of Health Guide for Care and Use of Laboratory Animals. Experiments were approved by the UCLA Chancellor's Animal Research Committee.

Experimental protocol – acute terminal and survival protocol (Figure 1 A, B)

Acute terminal experiment

To test the feasibility of reproducibly attenuating cardiac vagal control using CNA guided by gated high-frequency stimulation, 5 Yorkshire pigs (S&S Farms, Romana, CA) including 3 males and 2 females (45-50kg) were studied in an initial terminal protocol.

CNA was performed using a three-dimensional electroanatomic map (EAM) with the FlexAbility (Abbott, St. Paul, MN) catheter and EnSite Velocity mapping system (Abbott, St. Paul, MN)(**Supplemental Figure 1**). Baseline cardiac vagal responses were characterized by bilateral extracardiac vagal nerve stimulation (ECVNS) using high-resolution fluoroscopy using the Ziehm Vision RFD hybrid edition (Orlando, FL, USA) (**Figure 1C,D**), followed by gated high-frequency stimulation to detect left superior ganglionated plexi (LSGP). After attenuating the local LSGP gated high-frequency stimulation response by ablation, ECVNS was repeated and gated high-frequency stimulation was performed to detect right atrial ganglionated plexi (RAGP). RAGP ablation was performed until loss of ECVNS response was achieved. Afterward, animals were sacrificed by inducing ventricular fibrillation (VF), and hearts were rapidly excised to study ablation lesions and GPs.

Chronic GP Ablation Studies

The protocol included survival experiments (CNA) and terminal experiments 6 weeks later. In total, 16 Yorkshire pigs (8 male and 8 female) weighing 45-50kg were randomized to CNA (n=8) or sham ablation (n=8). Study animals subsequently underwent chronic terminal experiments as described.

In terminal experiments, baseline ECVNS responses were quantified, followed by gated high-frequency stimulation guided characterization of local GP responses. Next, bilateral vagi and sympathetic chains were stimulated. Finally, the left anterior descending coronary artery

(LAD) was ligated. After 10-minutes of observation, animals that did not develop VF were sacrificed as previously described.

Experimental protocol- definitions and settings

Gated HFS was performed using a Micropace EPS320 system (GE Health, Australia) with settings of 10mA, 50Hz, 5ms pw, 80-120ms total burst, and a pacing duration of 5 seconds **(Figure 1E)**. S1 represents the sensing channel, which uses high right atrial (HRA) signals acquired by a quadripolar catheter (Supreme, Abbott, St. Paul, MN). S2 denotes the time delay between sensing the HRA signal to starting HFS. S2 is adjusted based on the timing difference between the HRA and the mapping catheter. S3 denotes the stimulation frequency (maximal 20ms (50Hz)). HFS started with 120ms and subsequently decreased to 100ms then to 80ms if AF was triggered within three beats.

GP mapping began with gated high-frequency stimulation of the LSGP near the junction of the left pulmonary artery, left atrial appendage, and left pulmonary vein. After defining the LSGP, ablation was performed and followed by gated high-frequency stimulation over the RAGP area. The area being targeted was expanded based on positive responses to gated high-frequency stimulation until such responses could no longer be elicited. A positive was defined as >3% prolongation of cycle length reproducible between atrial signals. **(Figure 1F-1)** The responses included 1: fixed prolonged cycle length **(Figure 1F-2)**, 2: gradually increasing cycle length **(Figure 1F-3)**, and 3: cycle length prolonging initially and gradually decreasing **(Figure 1F-4)**.

Endpoints of CNA were the loss of local gated high-frequency stimulation response and loss of ECVNS response at the spot with the strongest response at baseline.

Supplemental methods and settings include animal anesthesia, hemodynamic data acquisition, electrocardiography (ECG), activation recovery interval (ARI), tissue collection, histologic studies, settings of ECVNS, CNA, thresholds acquiring, direct vagal nerve stimulation (VNS), and sympathetic chain stimulation (SCS).

Statistical analysis

All data are given as mean ± standard deviation and examined by the Shapiro-Wilk test for assessing normal distribution. Group comparisons were performed using the Student t-test for normal distribution data and the Wilcoxon signed-rank test for non-normally distributed data. When comparing groups >2, ANOVA was used if all the values were confirmed as normally distributed, or using a Kruskal-Wallis test for non-normal distributions. For all comparisons, $p<0.05$ was considered significant. Data were handled and analyzed using GraphPad Prism Version 9 (GraphPad Software, La Jolla, CA).

RESULTS

Despite complete loss of functional response, CNA does not eliminate all ganglia within the targeted plexus

Acutely following CNA, ECVNS-induced sinus rate slowing was abolished after 21±7.7 lesions applied to the LSGP and 13.5±1.9 lesions to the RAGP (left ECVNS-induced sinus rate slowing response at baseline vs. after CNA: -40.90 ± 35.8% vs. -2.54 ± 4.3%, p=0.044 and right ECVNS-induced response at baseline vs. after CNA: -35.62 ± 21.8% vs. 0%, p=0.001).

To examine the accuracy of gated high-frequency stimulation in detecting GPs and to test the effectiveness of CNA in eliminating all GPs in the targeted area, we performed the histologic

analysis of GPs following CNA. The approaches taken are shown in **Figure 2A, 2B**, and **Supplemental Figure 2**. Masson's trichome examinations showed that the ablated area was directly beneath 3 ganglia within the fat pad **(Figure 2C, 2E)** and 1 ganglion close to the myocardium **(Figure 2C, 2D)**. Of the 4 ganglia seen within the GP at the site of ablation in this example, only one near the myocardium was completely ablated as evidenced by loss of ganglion and neuron structure, as well as evidence of intra-ganglionic hemorrhage. Interestingly, the other larger ganglia were not physically impacted **(Figure 2F)** despite the confirmed loss of functional responses to GP stimulation and to ECVNS. In another animal, following extensive ablation of the RAGP, only 10 of 16 ganglia were fully ablated **(Supplemental Figure 2-3)**. Among all animals, bilateral ECVNS responses were attenuated with 54.5 ± 8.6% of examined ganglia in the plexus being ablated. This suggests that despite the confirmed functional elimination of local GP responses and loss of cardiac vagal inputs via GP, several ganglia remain. Similar findings were observed after examining LSGP following ablation near the LA posterior wall between the junction of the left pulmonary vein and the left pulmonary artery. However, in some animals, while left ECVNS responses decreased substantially (e.g. from 100% of maximal HR to 32%), it could not be completely eliminated despite extensive ablation **(Figure 2G-J)** and loss of responses to local gated high-frequency stimulation. This emphasizes the distributed network structure of cardiac GPs.

Effects of chronic CNA on vagal control of the sinus node and atrioventricular nodes (AVN)

In chronic studies, 16 animals were randomized to sham ablation or CNA with resulting attenuation of ECVNS-induced sinus rate slowing and PR prolongation effects **(Figure 3A, 3B) (Supplemental Table 1 & 2)** in the CNA group. After 6 weeks, we confirmed persistent loss of cardiac vagal input after CNA. Left ECVNS-induced sinus rate slowing remained attenuated (-35.69 ± 15.2% vs -7.21 ± 7.9%, p<0.001) after CNA **(Figure 3C, Right panel)**. Similarly, right ECVNS-induced sinus rate slowing remained attenuated (-29.49 ± 16.4% vs. -5.64 ± 6.8%, p=0.018) after CNA **(Figure 3D, right panel)**. In sham CNA animals, sinus rate slowing induced by bilateral ECVNS remained unchanged. **(Supplemental Table 3) (Figure 3C, 3D, left panel)**

To examine the effect of CNA on attenuating vagal control of AVN, the PR interval before and immediately after ECVNS were analyzed. In controls, the PR interval increased by 35.34 ± 11.8% and 23.33 ± 7.2% after left ECVNS and right ECVNS respectively and remained consistent throughout the procedure and after 6 weeks. **(Figure 3E, 3F, left panel)** In ablated animals, bilateral ECVNS-induced PR interval prolongation was attenuated significantly by CNA and the effect persisted for at least 6 weeks. Specifically, left ECVNS-induced PR interval prolongation decreased from 36.15 ± 26.8% to 7.02 ± 5.3 % with a p-value of 0.040, and right ECVNS-induced PR interval prolongation decreased from 23.73 ± 11.3% to 6.54 ± 6.2% with a p-value of 0.014 **(Figure 3E, 3F, right panel) (Supplemental Table 1)**. Additionally, the resting PR interval shortened significantly from 125.40 ± 10.2ms to 95.61± 12.0ms after CNA. Further, while left ECVNS-induced AVB was noted in 87.5% in controls and 0% in CNA animals with a p-value of 0.005 **(Figure 3G)**. These findings indicate that targeting LSGP and

RAGP is sufficient to attenuate the vagal control of AVN, even though the inferior vena cava-interatrial GP is more commonly associated with AV nodal control.

Next, we examined the impact of chronic CNA on sinus nodal control. Activation mapping of the sinus node complex in chronic CNA animals compared to controls showed an interesting shift in the pacemaker site to the inferior right atrium, adjacent to the IVC-RA junction in 6/8 animals while only 1/8 animals in the sham ablation group showed this activation pattern with a p-value of 0.014. **(Figure 4)**

Chronic CNA effects extend beyond sinus node and AVN control and causes cardiovascular autonomic dysreflexia

To examine cardiovascular reflex response after CNA, hemodynamic measures were recorded while direct VNS and SCS were performed. There was a 10-fold increase in direct VNS stimulation current required to induce a 10% sinus rate slowing effect in the ablation group **(Figure 5A-C)**. In sham ablated animals, direct VNS (mean stimulation current of 1.28 ± 0.3mA for direct right VNS and 1.20 ± 0.7 mA for direct left VNS) resulted in the expected physiological response of HR slowing and decreased left ventricular systolic pressure (LVSP). However, in CNA animals, direct VNS (mean stimulation current of 11.48 ± 5.3mA in direct right VNS and 13.39 ± 4.6mA in direct left VNS) resulted in paradoxical increases in HR during stimulation. **(Figure 5A, 5D, 5F).** Additionally, rather than a physiologic reduction in LVSP, direct VNS induced a mean of 5-10% LVSP increase in CNA animals. **(Supplemental Table 4) (Figure 5E, 5G)**. Analysis of dp/dt change also showed the paradoxical increase in CNA animals. **(Supplemental Figure 4)**

Direct SCS demonstrated similar thresholds of RSCS and LSCS. In controls, RSCS with 4Hz and 8Hz increased HR by 26.16 ± 16.6% and 41.21 ± 24.7%, and increased LVSP by 6.23 ± 3.9% and 6.63 ± 5.1% respectively. In the ablated animals, RSCS induced a similar HR increase compared with controls, however, the LVSP responses at 4Hz and 8Hz were attenuated with a change of 2.60 ± 2.7% and 1.65 ± 3.1% with a p-value of 0.231 and 0.033 comparing with the controls. **(Figure 6D-E)**

Importantly, LSCS resulted in LVSP increase with a physiological (baroreflex mediated) decrease in HR in controls, but this HR decrease response was not seen in CNA animals (Figure 6A), rather, there was a paradoxical HR increase in ablated animals. **(Supplemental Table 5) (Figure 6F, 6G)**

These paradoxical responses in blood pressure and heart rate indicated that the effects of CNA extend beyond sinus and AV nodal control to impact baroreflex sensing mechanisms and impact cardiovascular reflexes more globally.

CNA enhances susceptibility to ischemia-induced VT/VF by disrupting repolarization dynamics

To evaluate the repolarization disturbance resulting from CNA, the QTc intervals and QTc dispersion were examined. We found that the baseline QTc intervals and QTc dispersion before CNA and sham procedure were similar in both groups. In controls, the QTc interval and QTc dispersion remained similar after the sham procedure with a mean change of 0.26 ± 3.6% and 21.39 ± 60.6% respectively. On the contrary, the QTc interval and QTc dispersion increased significantly after CNA by 9.98 ± 4.2% and 160.94 ± 106.4%. **(Figure 7A-C)** After 6 weeks, the baseline QTc remained prolonged, and QTc dispersion remained increased in the ablation group

(Figure 7D). Importantly, the impact of CNA on ventricular repolarization not only exists in a resting status by also in sympathetic stimulation. In controls, LSCS at 4Hz and 8Hz increased QTc by 2.76% and 1.49%, but this QT prolongation effect was enhanced in CNA animals with an 8.19 and 11.23% increase. During RSCS, the controls demonstrated QTc shortening responses, but the ablation group showed a paradoxical QTc prolongation. **(Supplemental Table 6, Supplemental Figure 5) (Figure 7E, 7F)**

To test whether CNA attenuates the vagal protective effect on ventricles, LAD ligation was performed. In ablated animals, the time to demonstrate PVC and NSVT after LAD ligation was significantly shorter than in controls. **(Figure 8A-E)** There was also a higher incidence of VF in the CNA animals (control vs. ablation: 25.0% vs 62.5%, p= 0.143), a significantly higher PVC burden within three minutes after LAD ligation, a higher percentage of polymorphic NSVT episodes (control vs. ablation: 14.3% vs. 66.7%, p= 0.039), and more NSVT episodes in ten minutes (controls vs ablation: 2.25 ± 2.5 vs 8.63 ± 6.1 episodes, p=0.011) **(Figure 8F-H)**. ARI shortening after 2 minutes of LAD ligation was greater in the ablation group. **(Supplemental Table 7) (Figure 8I)** The enhanced susceptibility to ischemic-induced VT/VF after CNA might be the result of cardiac vagal denervation, autonomic dysreflexia, and disrupted repolarization dynamics.

DISCUSSION

The principal findings in this study are (1) gated high-frequency stimulation can guide CNA and complete GP ablation is not a prerequisite for attenuating cardiac vagal control, (2) LSGP and RAGP ablation modulate vagal control of sinus node and AVN and the effect persists

after 6 weeks and (3) CNA results in cardiovascular autonomic dysreflexia and increases the susceptibility to ventricular arrhythmias in the setting of ischemia, potentially by interfering with ventricular repolarization. (Central Illustration) CNA as a novel therapy for VVS is gaining popularity. Its intermediate and long-term safety is unknown. To the best of our knowledge, here we present the first chronic animal model of CNA to evaluate the long-term effects of CNA in detail.

Physiological function of Cardiac GP

GPs exert final vagal control on the heart. The distributed network of GPs within epicardial fat pads comprises the intrinsic cardiac nervous system, capable of cardio-cardiac reflexes thought to involve both parasympathetic and sympathetic neurons.[7] Currently, there is no agreement on which GPs to target in clinical studies. Four GPs are commonly targeted clinically, including RAGP (right atrium GP or right anterior GP), LSGP, left inferior GP (LIGP), and right inferior GP (RIGP) **(Figure 2L)**.[3,8]

In this study, we targeted RAGP and LSGP since both GPs are reported to show bradycardia or tachycardia responses during ablation. [9,10] Interestingly, targeting these two GPs alone abolished vagal control of both the SA and AV nodes. This suggests that the LIGP, analogous to the IVC-inferior left atrial (IVC-ILA) GP in humans, often associated with the AV node, may not be required to modulate the AV node. This is important as the IVC-ILA GP is near the cardiac conduction system. Further, since the intrinsic cardiac nervous system is a distributed network of interconnected GPs, our findings suggest that targeting these two GPs

alone may impact the network function of GPs to exert additional effects beyond the regions typically subtended by these two GPs.

Intraprocedural methods to identify GPs

There is currently no standardized methodology for identifying GPs intraprocedurally. Current methods include endocardial or surgical HFS[10], customized software to target the fragmented atrial signals, and empirical anatomical approaches.[8] Importantly, histologic proof of GP existence at ablated sites is limited or absent in most studies as this can only be obtained postmortem.[11]

We performed gated high-frequency stimulation with a built-in Refractory-HFS program in a commercially available system during the atrial refractory period to avoid triggering AF.[12] The gated high-frequency stimulation-guided ablation lesions were excised to confirm the existence of GPs and to assess the impact of ablation. Additionally, intraprocedural confirmation of centrifugal responses to gated high-frequency stimulation i.e., as stimulation moves away from the GP, the response to stimulation gradually decreases, provided further evidence of GP localization. This finding is consistent with our histologic data showing that the GPs exist in a relatively focal site, as opposed to sporadic distribution, as previously published [13].

Chronic effects of CNA on cardiac vagal control of the SA node

The subacute effects of CNA have not been systematically evaluated prior to this chronic porcine model of CNA. We showed that ECVNS-mediated HR slowing and PR prolongation effects were maintained 6 weeks after CNA. Importantly, ECVNS-mediated AVB was not seen in the ablation group, emphasizing the efficacy of targeting LSGP+RAGP. It should be noted that

HR slowing, and PR prolongation effects increased over time in both groups, indicating that when ECVNS was used as a procedure endpoint, how much destruction of GP is required to achieve the endpoint may vary with the maturity of the subject. Additionally, given the fact that half of the ganglia was not ablated during a CNA, ECVNS responses might recover. Unlike recovery after ablation of nerve fibers, ablation of neuronal soma (cell body) is irreversible thus the recovery could be probably contributed to nerves sprouting from the remaining ganglia to reach the SA node and AV node.

Activation mapping of the sinus node in sham and chronic CNA animals showed an interesting caudal shift in the site of earliest activation in ablated but not sham animals. Likely a result of disrupting the connection between the RAGP and sinus node [14], this finding provides an important insight into the mechanisms by which CNA exerts its effects. It suggests that the RAGP not only acutely mediates vagal neurotransmission to the SA node, it tonically maintains the functional architecture of the SA node. Since both sham and chronic CNA animals exhibited similar HR increases to sympathetic stimulation, it does not appear that this shift impacts chronotropic reserve within the SA node. Propagation patterns from the earliest site of activation in the SA nodal complex appeared similar between sham and chronic CNA animals suggesting that the transitional zone is not impacted by RAGP ablation.

CNA results in cardiovascular autonomic dysreflexia

We observed that compared to uniform reductions in HR in sham ablation animals, chronic CNA animals exhibited an initial HR reduction followed by a significant increase above baseline. This unexpected paradoxical HR increase during direct VNS likely reflects afferent reflex responses to VNS, as the vagus nerve mediates both afferent and efferent

neurotransmission. Since the efferent vagal control on the heart has been abolished by CNA, it leaves afferent neurotransmission unperturbed. The enhanced vagal afferent signaling might thereby activate sympathetic efferent signaling and result in HR increase. This response was limited to direct VNS but not ECVNS, likely due to the complex nature of ECVNS that is not seen in direct stimulation of the vagus nerve using cuff electrodes. Specifically, by stimulating a large region within the neurovascular bundle, ECVNS activates the sympathetic chain and vagus nerve, but likely also impacts fibers of the carotid sinus which is known to be sympathoinhibitory (during baroreflex activation). Direct VNS also induced a paradoxical increase in LVSP compared with sham animals. Similar to HR responses, this finding is likely explained by afferent-mediated reflex sympathetic responses following CNA. However, it highlights the important point that the chronic effects of CNA extend beyond SA and AV nodal responses to cardiac contractile responses and LV pressure responses.

Dysreflexic responses were also observed during sympathetic stimulation. Typically, RSCS always increases HR, while LSCS exhibits a reduction (likely via baroreflex), no change, or less frequently an increase in HR. Specifically, LVSP increases were lower in chronic CNA animals compared to sham ablated animals during RSCS, which may be related to chronic structural and or functional remodeling of cardiac sympathetic signaling after CNA. Additionally, via baroreflex responses, LSCS resulted in a compensatory reduction in HR in sham animals, however, in chronic CNA animals, HR increased. This paradoxical might be explained by that CNA attenuates cardiac vagal control and thereby eliminates the “brake” during sympathoexcitation. This finding is of great importance given the fact that depressed baroreflex sensitivity has been shown to carry a higher risk of sudden cardiac death. In totality, the findings indicate more extensive dysreflexia than previously appreciated after CNA and

emphasize the complex functions of the intrinsic cardiac nervous system and autonomic responses to CNA.

Impact of chronic CNA on VAs susceptibility and ventricular repolarization

Sparse data indicate that PVI is associated with varying degrees of GP ablation and may be associated with PVCs, electrical storms, or takotsubo cardiomyopathy. [15-17] Although acute studies in rodents suggest that withdrawal of vagal activity following partial atrial denervation increases the susceptibility to VAs [6,18], data from a contemporary CNA model is lacking.

We found that the QTc interval increased significantly after CNA, while it remained unchanged in sham animals, and this effect persisted at 6 weeks. This finding suggests that partial vagal denervation during PVI may explain QTc prolongation in some patients after PVI. [6,19] However, conflicting results were reported. [20] These could be explained by the approaches of CAN which GP was defined as the fragmented signals and the endpoint is signal attenuation rather than ECVNS. Whether the ECVNS effect was attenuated in prior studies is unknown. Additionally, the study hypothesized the effect of QTc shortening is caused by sympathetic denervation. This hypothesis, however, was not compatible with our results showing clearly that sympathoexcitation was not impacted after a successful CNA. Finally, we should point out that this may reflect a species difference: mouse vs pig vs human. Additionally, QTc dispersion, a marker of repolarization heterogeneity, increased after CNA [21] in line with previous clinical observations that QTc dispersion increased in patients with increased PVCs after PVI.[16] This line of reasoning raises questions about the safety of CNA in patients at high risk of VAs.

Strikingly, we found that CNA resulted in a significantly higher susceptibility to VAs, including earlier PVC, NSVT, and VF, a higher burden of VAs, and a higher incidence of

polymorphic NSVT. In addition, while LAD ligation resulted in equivalent infarct size in sham and CNA animals, ventricular ARI shortening was greater in the CNA group compared to the sham. The shortening in this surrogate marker of action potential duration in CNA vs. sham animals likely reflects the greater adrenergic surge in response to myocardial ischemia.[22] These novel findings illustrate that CNA not only eliminates the vagal control of the atrium, but it also diminishes the cardioprotective effect of vagal signaling in the ventricular myocardium.

Limitations

Several limitations should be noted. (1) The procedure was performed in a healthy swine and should be translated with caution into humans who may have evidence of vagal dysfunction contributing to their SA or AV nodal dysfunction. Currently, there are no clear data regarding pathophysiological alterations in GP of patients with VVS, thus it remains unknown if CNA impacts dysfunctional GPs or eliminates GPs to treat a different etiology. (2) Optimal methods to identify GP, metrics for procedural endpoints, approaches to test vagal inputs to the heart, and efficacy of GP ablation (i.e. extensive vs limited) remain controversial. Thus, the effect of complete GP ablation was not studied here. However, the current study demonstrated that ablating all GP is neither feasible nor a prerequisite for achieving the functional clinical endpoints used in most studies. (3) The highest stimulation frequencies studied ranged 30-50Hz. Whether higher frequency stimulation would affect the results and endpoints remains unclear. Nevertheless, the high-frequency stimulator, e.g., the Grass stimulator, is not readily available in most clinical cardiac catheterization labs. (4) Telemetry was not implanted to assess the chronic ventricular arrhythmias during the 6-week recovery period. (5) The hypothesis of sympathetic reflex-related paradoxical HR and BP response during VNS was not confirmed by transecting the

sympathetic chain or administration of beta-adrenergic receptor blockers. Additionally, examination of the stellate ganglion may identify changes that suggest functional changes at the level of the stellate ganglion.

Conclusions

In this chronic CNA porcine model, we demonstrated that local cardiac vagal denervation reaching several clinical endpoints can be achieved and maintained for at least 6 weeks despite incompletely ablating the ganglia. Importantly, CNA effects extended beyond sinus node and AVN control to reflex vagal and sympathetic dysreflexia, and to the interaction between the two. CNA also impacted ventricular repolarization and diminished the cardioprotective effect of cardiac vagal input to the ventricles by enhancing susceptibility to VAs. This finding highlights the potential negative impact of CNA as an iatrogenic cause of cardiac autonomic dysregulation and ischemia-induced VAs.

References

1. Arora RC, Waldmann M, Hopkins DA, Armour JA. Porcine intrinsic cardiac ganglia. Anat Rec A Discov Mol Cell Evol Biol 271(1):249-258, 2003
2. Scherlag BJ, Yamanashi WS, Schauerte P, Scherlag M, Sun YX, Hou Y, Jackman WM, Lazzara R. Endovascular stimulation within the left pulmonary artery to induce slowing of heart rate and paroxysmal atrial fibrillation. Cardiovasc Res 54(2):470-475, 2002
3. Huang X, Chen Y, Huang Y, Zhao H, He L, Tan Z, Xu D, Peng J. Comparative effects of intensive ganglionated plexus ablation in treating paroxysmal atrial fibrillation and vasovagal syncope. Clin Cardiol 43(11):1326-1333, 2020
4. Pachon JC, Pachon EI, Pachon JC, Lobo TJ, Pachon MZ, Vargas RN, Jatene AD. "Cardioneuroablation"--new treatment for neurocardiogenic syncope, functional AV block and sinus dysfunction using catheter RF-ablation. Europace 7(1):1-13, 2005
5. Piotrowski R, Baran J, Sikorska A, Krynski T, Kulakowski P. Cardioneuroablation for Reflex Syncope: Efficacy and Effects on Autonomic Cardiac Regulation-A Prospective Randomized Trial. JACC Clin Electrophysiol 9(1):85-95, 2023
6. Jungen C, Scherschel K, Eickholt C, Kuklik P, Klatt N, Bork N, Salzbrunn T, Alken F, Angendohr S, Klene C, Mester J, Klocker N, Veldkamp MW, Schumacher U, Willems S, Nikolaev VO, Meyer C. Disruption of cardiac cholinergic neurons enhances susceptibility to ventricular arrhythmias. Nat Commun 8:14155, 2017
7. Armour JA. Cardiac neuronal hierarchy in health and disease. Am J Physiol Regul Integr Comp Physiol 287(2):R262-271, 2004
8. Debruyne P, Rossenbacker T, Janssens L, Collienne C, Ector J, Haemers P, le Polain de Waroux JB, Bazelmans C, Boussy T, Wijns W. Durable Physiological Changes and Decreased Syncope Burden 12 Months After Unifocal Right-Sided Ablation Under Computed Tomographic Guidance in Patients With Neurally Mediated Syncope or Functional Sinus Node Dysfunction. Circ Arrhythm Electrophysiol 14(6):e009747, 2021
9. Baysal E, Guler TE, Gopinathannair R, Bozyel S, Yalin K, Aksu T. Catheter Ablation of Atrioventricular Block: From Diagnosis to Selection of Proper Treatment. JACC Case Rep 2(11):1793-1801, 2020
10. Yao Y, Shi R, Wong T, Zheng L, Chen W, Yang L, Huang W, Bao J, Zhang S. Endocardial autonomic denervation of the left atrium to treat vasovagal syncope: an early experience in humans. Circ Arrhythm Electrophysiol 5(2):279-286, 2012
11. Onorati F, Curcio A, Santarpino G, Torella D, Mastroroberto P, Tucci L, Indolfi C, Renzulli A. Routine ganglionic plexi ablation during Maze procedure improves hospital and early follow-up results of mitral surgery. J Thorac Cardiovasc Surg 136(2):408-418, 2008

12. Schauerte P, Mischke K, Plisiene J, Waldmann M, Zarse M, Stellbrink C, Schimpf T, Knackstedt C, Sinha A, Hanrath P. Catheter stimulation of cardiac parasympathetic nerves in humans: a novel approach to the cardiac autonomic nervous system. Circulation 104(20):2430-2435, 2001
13. Kim MY, Coyle C, Tomlinson DR, Sikkel MB, Sohaib A, Luther V, Leong KM, Malcolme-Lawes L, Low B, Sandler B, Lim E, Todd M, Fudge M, Wright IJ, Koa-Wing M, Ng FS, Qureshi NA, Whinnett ZI, Peters NS, Newcomb D, Wood C, Dhillon G, Hunter RJ, Lim PB, Linton NWF, Kanagaratnam P. Ectopy-triggering ganglionated plexuses ablation to prevent atrial fibrillation: GANGLIA-AF study. Heart Rhythm 19(4):516-524, 2022
14. Bychkov R, Juhaszova M, Calvo-Rubio Barrera M, Donald LAH, Coletta C, Shumaker C, Moorman K, Sirenko ST, Maltsev AV, Sollott SJ, Lakatta EG. The Heart's Pacemaker Mimics Brain Cytoarchitecture and Function: Novel Interstitial Cells Expose Complexity of the SAN. JACC Clin Electrophysiol 8(10):1191-1215, 2022
15. Patel PJ, Ahlemeyer L, Freas M, Cooper JM, Marchlinski FE, Callans DJ, Hutchinson MD. Outflow tract premature ventricular depolarizations after atrial fibrillation ablation may reflect autonomic influences. J Interv Card Electrophysiol 41(2):187-192, 2014
16. Munkler P, Wutzler A, Attanasio P, Huemer M, Parwani AS, Haverkamp W, Meyer C, Boldt LH. Ventricular Tachycardia (VT) Storm After Cryoballoon-Based Pulmonary Vein Isolation. Am J Case Rep 19:1078-1082, 2018
17. Liu X, Chen X, Li X, Ma C. Takotsubo syndrome following radiofrequency ablation of atrial fibrillation in a patient with coronary artery anomaly: a case report. Eur Heart J Case Rep 6(4):ytac147, 2022
18. He B, Lu Z, He W, Wu L, Cui B, Hu X, Yu L, Huang C, Jiang H. Effects of ganglionated plexi ablation on ventricular electrophysiological properties in normal hearts and after acute myocardial ischemia. Int J Cardiol 168(1):86-93, 2013
19. Chikata A, Kato T, Usuda K, Fujita S, Maruyama M, Otowa KI, Usuda K, Niwa S, Tsuda T, Hayashi K, Takamura M. Prolongation of QT interval after pulmonary vein isolation for paroxysmal atrial fibrillation. J Cardiovasc Electrophysiol 31(9):2371-2379, 2020
20. Aksu T, Guler TE, Bozyel S, Golcuk SE, Yalin K, Lakkireddy D, Gopinathannair R. Medium-term results of cardioneuroablation for clinical bradyarrhythmias and vasovagal syncope: effects on QT interval and heart rate. J Interv Card Electrophysiol 60(1):57-68, 2021
21. Somberg JC, Molnar J. Usefulness of QT dispersion as an electrocardiographically derived index. Am J Cardiol 89(3):291-294, 2002
22. Millar CK, Kralios FA, Lux RL. Correlation between refractory periods and activation-recovery intervals from electrograms: effects of rate and adrenergic interventions. Circulation 72(6):1372-1379, 1985

Figure 1. Experimental design and high-frequency stimulation settings

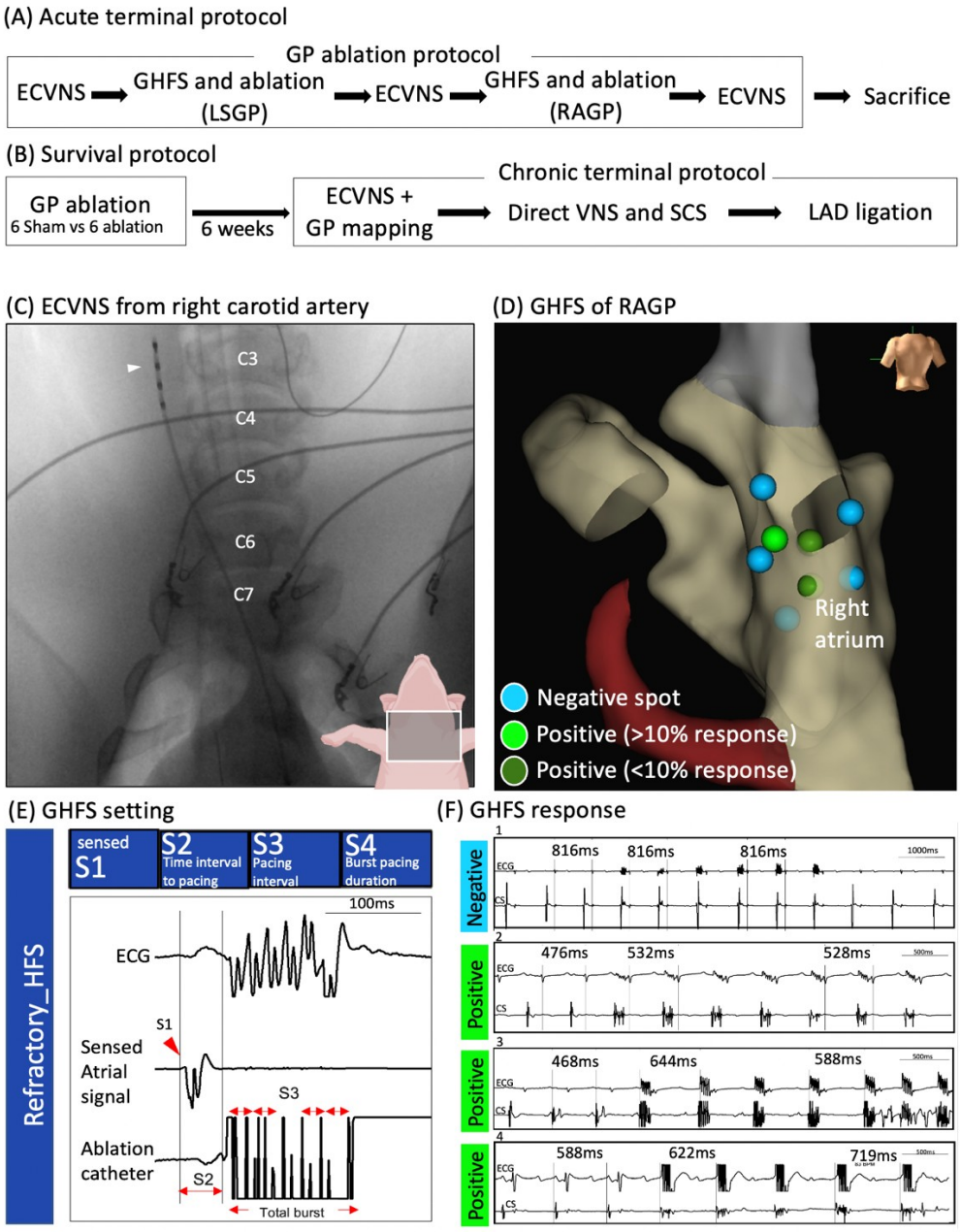

(A) shows the steps of cardioneuroablation (CNA). (B) shows the survival protocol comprising CNA and chronic terminal protocol. (C) shows intracarotid vagal nerve stimulation by a quadripolar catheter (white arrowhead) to stimulate inside the right carotid artery next to C-spine level 3 and 4. (D) shows the centrifugal distribution of the positive spots of gated high-frequency stimulation (E) shows the setting of Micropace EPS320 system with the Refractory_HFS protocol. The red arrowhead indicates the sensed atrial signal. (F) shows negative (1) and

positive (2-4) responses to gated high-frequency stimulation. In the negative response, HR does not change. The second to fourth figures show the constant, decremental, and incremental response respectively. ECVNS= extracardiac vagal nerve stimulation; LSGP= left superior ganglionated plexi; SCS= sympathetic chain stimulation.

Figure 2. RAGP and LSGP electroanatomic mapping (EAM) and histology

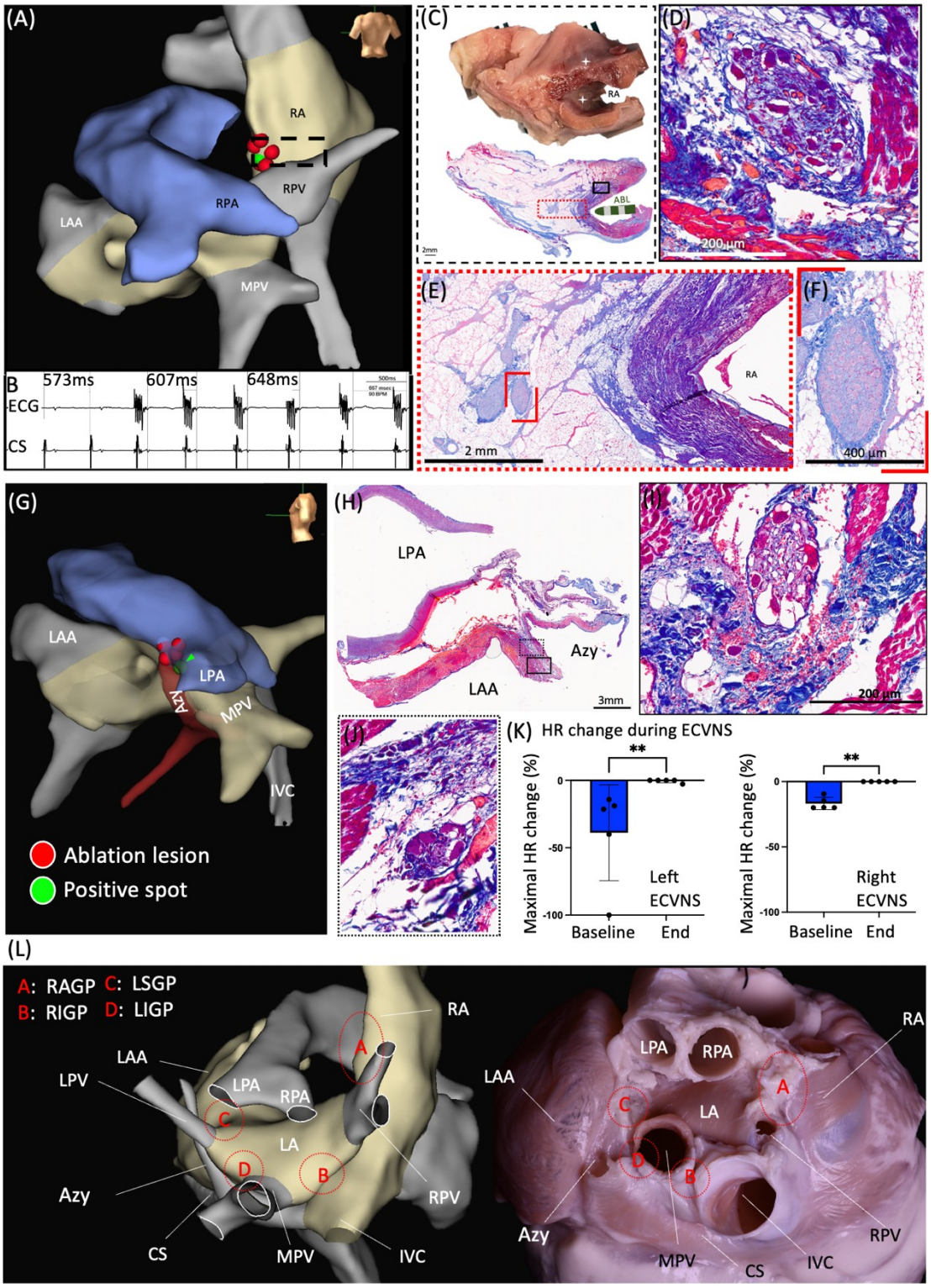

(A)(G) show the positive spots detected by gated high-frequency stimulation over right atrial ganglionated plexi (GP)(A) and left superior ganglionated plexi (G) (green arrowhead) areas. (C-F, H-J) show the ablated GP (D, I) and the intact GP (F, J). Note that the extracardiac vagal nerve stimulation effect was attenuated (K) despite residual intact GP. (L) showed the EAM and the correlation in a pressure-fixation porcine heart. **p<.01. Azy= azygos vein; CS= coronary sinus; IVC= inferior vena cava; LA= left atrium; LAA= left atrial appendage; LIGP= left inferior ganglionated plexi; LPA= left pulmonary artery; LSGP= left superior ganglionated plexi; MPV= middle pulmonary vein; RA= right atrium; RIGP= right inferior ganglionated plexi; RPV= right pulmonary vein; RPA= right pulmonary artery.

Figure 3. Cardioneuroablation effect on sinus node and atrioventricular node

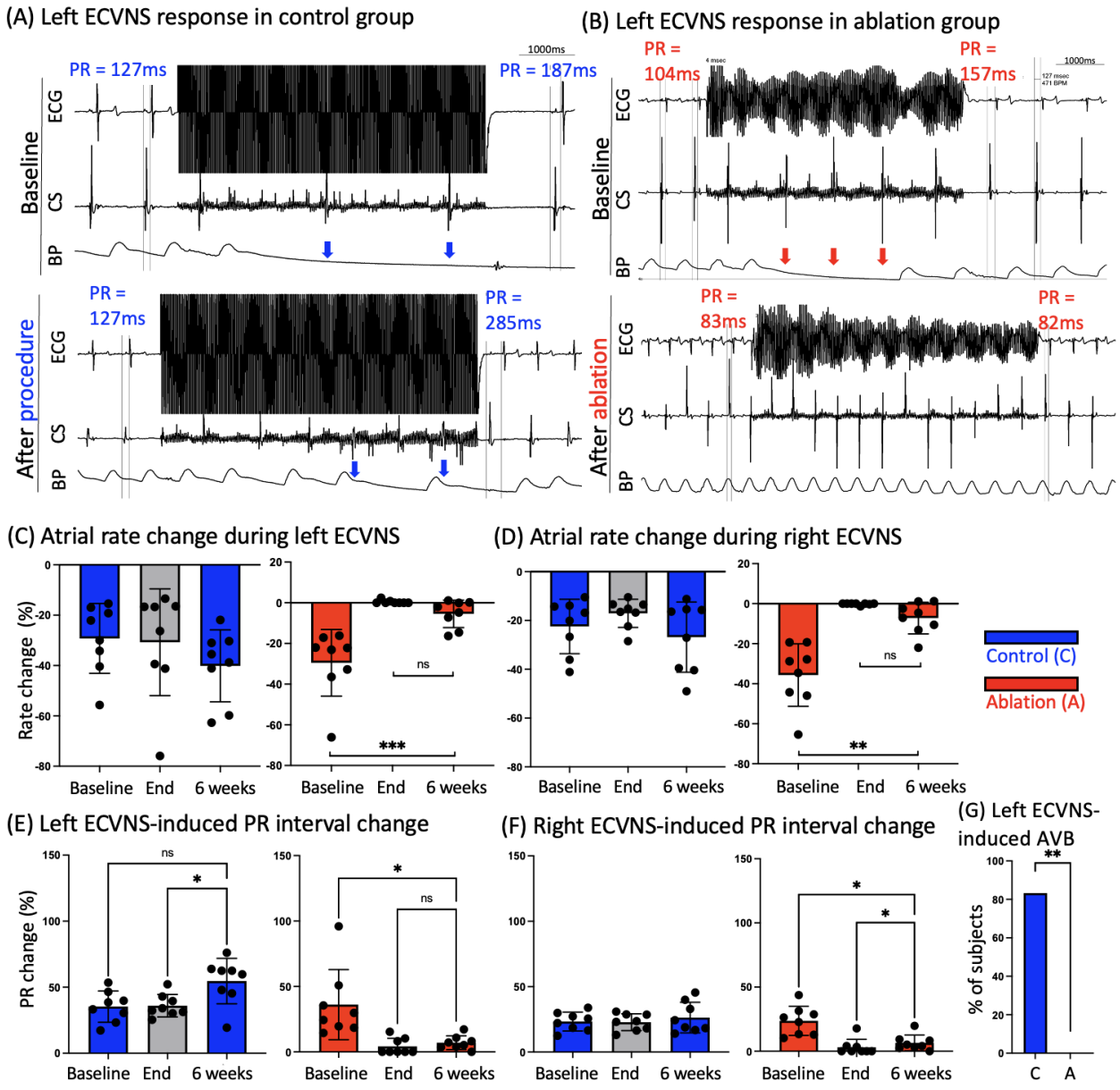

(A)(B) show atrioventricular block (arrow) and atrial rate (HR) slowing response induced by extracardiac vagal nerve stimulation (ECVNS) remained consistent throughout the sham procedure but the effect was attenuated after cardioneuroablation. (C-F) show that the ECVNS-induced atrial rate change (C, D) and PR interval change (E, F) remained similar in controls (left panel) but were attenuated acutely after cardioneuroablation and persisted for at least 6 weeks.

(Right panel). (G) shows a higher incidence of the atrioventricular block during left vagal nerve stimulation in controls but none in the ablation group. *p <.05; **p<.01; ***p<.001; 6 weeks = 6 weeks after survival procedure; AVB = atrioventricular block, BP = blood pressure; CS = coronary sinus; ECVNS= extracardiac vagal nerve stimulation; End = end of the survival procedure.

Figure 4. Activation map 6 weeks after cardioneuroablation

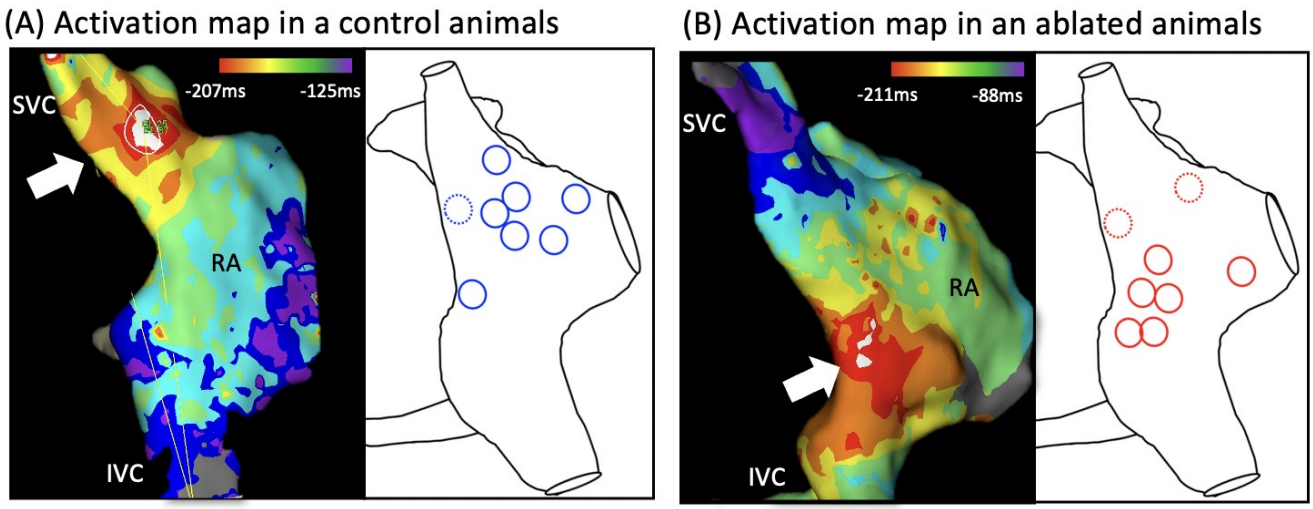

Shows the earliest activation area (white arrow) in each group 6 weeks after the procedure. The scheme shows the collective result of the earliest activation site in 8 animals in each group. Note that in controls, the earliest activation was located closer to the SVC-RA junction.. In ablated animals, the activation demonstrated a caudal shift of the earliest activation. The dotted line = the earliest activation is located at the septal site. IVC= inferior vena cava, LA= left atrium; RA= right atrium; SVC= superior vena cava.

Figure 5. Hemodynamic change during direct vagal nerve stimulation (VNS)

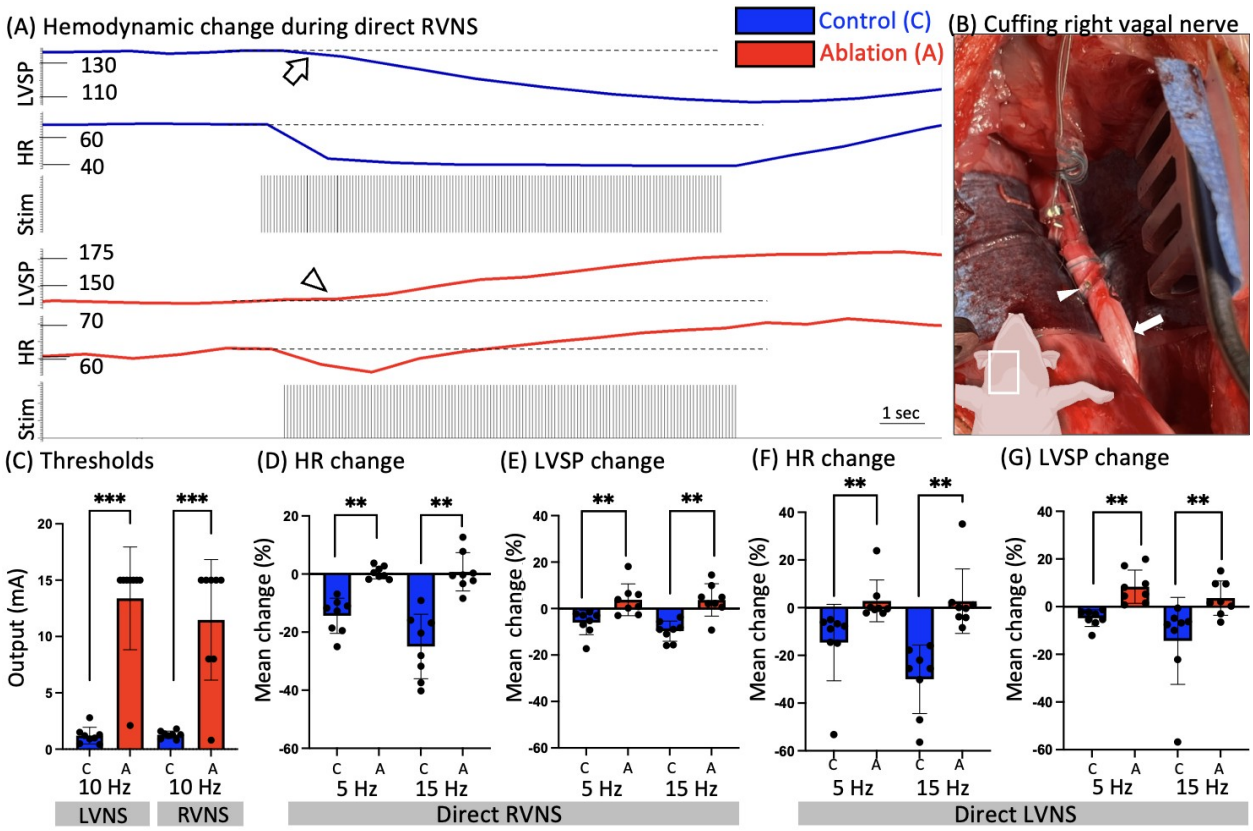

(A) shows heart rate (HR) and left ventricular systolic pressure (LVSP) decreasing during direct right VNS in controls. Note that LVSP decreased (clear arrowhead) after HR decreased. In the ablation group, HR decreased initially, then increased above baseline and LVSP (clear arrowhead) throughout direct right VNS. (B) shows the platinum cuff (solid arrowhead) wrapping the right vagal nerve (solid arrow). (C) shows the thresholds increased significantly in the ablation group. (D-G) show that HR change approximates 0% with paradoxical LVSP increase in ablated animals. **p<.01; HR=heart rate; LVSP = left ventricular systolic pressure; LVNS= left vagal nerve stimulation; RVNS= right vagal nerve stimulation.

Figure 6. Hemodynamic change during direct sympathetic chain stimulation (SCS)

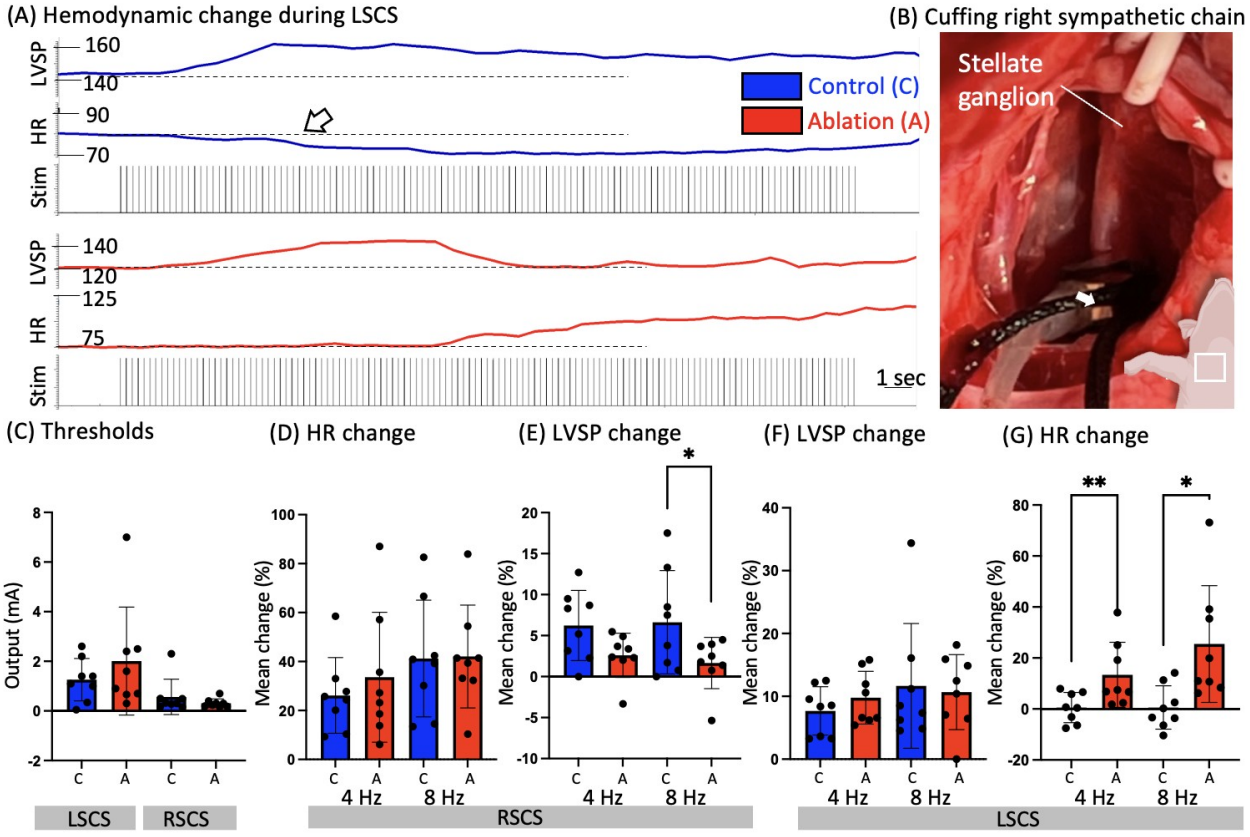

(A) shows heart rate (HR) decreases (clear arrow) during left sympathetic chain stimulation (SCS) in controls but increased in the ablation group. (B) shows the platinum cuff (arrow) wrapping the right sympathetic chain distal to the stellate ganglion. (C) Shows insignificant higher thresholds of LSCS in the ablation group. (D-G) During right SCS, HR increased similarly, but blood pressure was lower in the ablation group. During left SCS, blood pressure increased similarly, but HR was higher in the ablation group. HR= heart rate; LSCS= left sympathetic chain stimulation; LVSP = left ventricular systolic pressure; RSCS= right sympathetic chain stimulation.

Figure 7. Cardioneuroablation results in QTc interval change

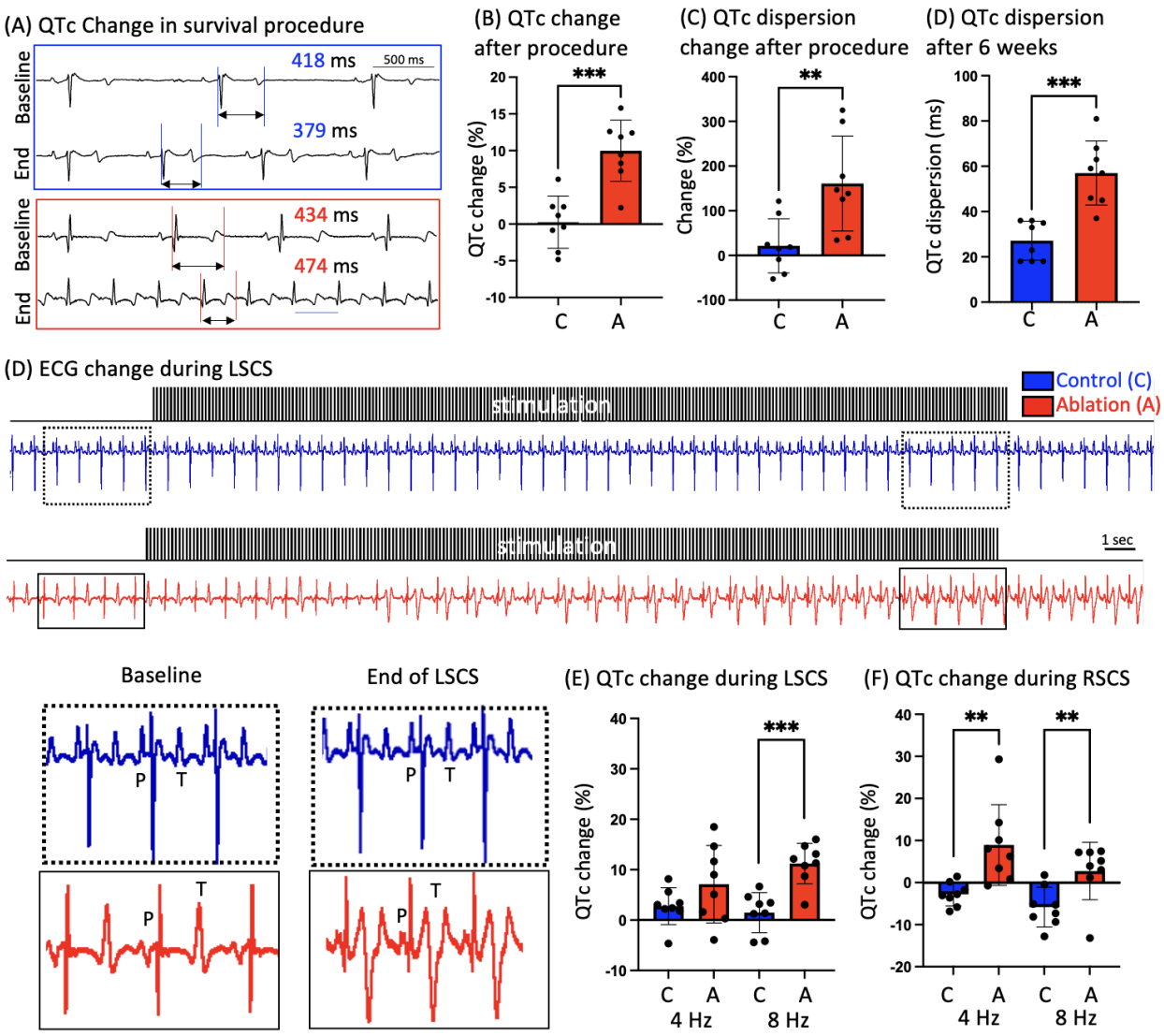

(A-C) show the QTc interval and dispersion increased significantly in the ablation group. QTc remained prolonged for 6 weeks. (D-F) show the QTc interval increased significantly during left sympathetic chain stimulation in ablated animals. QTc interval shortens during right sympathetic chain stimulation in controls but prolongs in ablated animals. Note that in the magnified electrocardiography, left sympathetic chain stimulation resulted in a significant T wave change and QTc prolongation in the ablation group. **p<.01; ***p<.001; LSCS= left sympathetic chain stimulation; RSCS= right sympathetic chain stimulation.

Figure 8. Ventricular arrhythmia susceptibility to ischemia

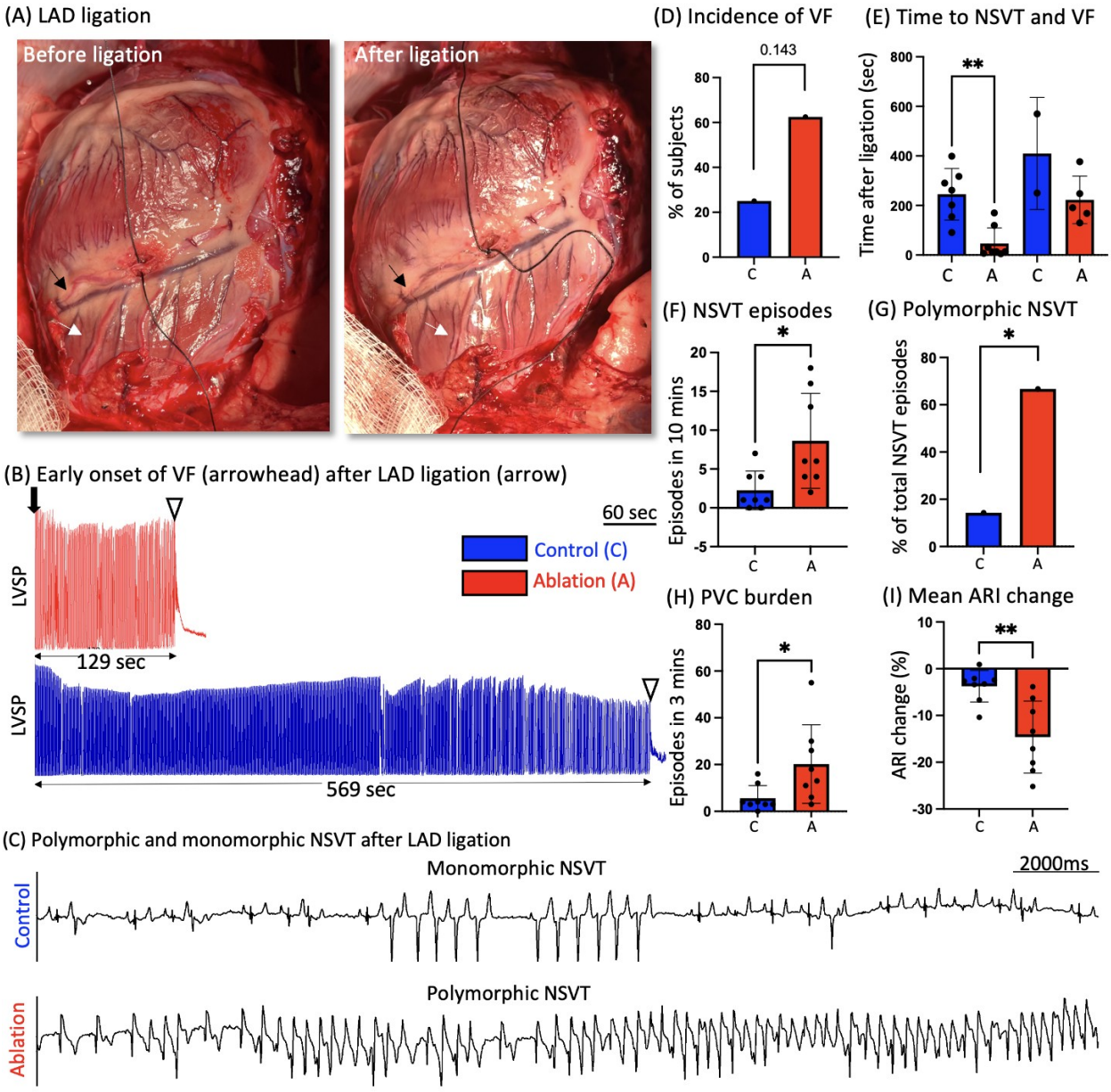

(A) shows the left anterior descending coronary artery (LAD) being ligated between two diagonal branches resulting in an ischemic change of the 2nd diagonal branch (thin white arrow) and distal LAD (thin black arrow). (B, D) show a shorter time to develop ventricular fibrillation (VF) (clear arrowhead) and higher incidence of VF in the ablation group. (C, E, F, G) show a predominance of polymorphic non-sustained

ventricular tachycardia (NSVT) and earlier onset of NSVT in the ablation group. (H) shows higher episodes of PVC. (I) shows a greater degree of activation recovery interval shortening in ablated animals. *p<.05; **p<.01; ARI = activation recovery interval; LVSP = left ventricular systolic pressure; NSVT = non-sustained ventricular tachycardia; PVC = premature ventricular complex.